Determining Loads for Down-scaled Testing of Wind Turbine Pitch Bearings using an Augmented Kalman Filter and Reference Measurements

Nathan Dwek, Daniel de Gregoriis, Mireia Olave, Matteo Kirchner, Frank Naets

Determining Loads for Down-scaled Testing of Wind Turbine Pitch Bearings using an Augmented Kalman Filter and Reference Measurements

Nathan DWEK[1,2], Daniel DE GREGORIIS[3], Mireia OLAVE[4], Matteo KIRCHNER[1,2], Frank NAETS[1,2]

[1]LMSD section, Department of Mechanical Engineering, KU Leuven, Belgium
[2]Flanders Make@KU Leuven, Leuven, Belgium
[3]Siemens Industry Software NV, Belgium
[4]IKERLAN, Spain
nathan.dwek@kuleuven.be

Abstract

This article proposes an approach to determine the loads to apply during down-scaled testing of wind turbine (WT) pitch bearings. Down-scaled testing consists in using already existing smaller test-rigs as part of the design and validation of new larger bearings. It allows to accelerate the development of WT pitch bearings and reduce the testing costs. It also poses the problem of which loads to apply on the down-scaled bearing in order to reproduce the fatigue life and defect formation of the larger reference bearing. The goal of this work is that down-scaled testing replicates strains at key locations around a failure mode of interest, so that the testing outcomes are representative of the operation of the reference bearing. To this end, an Augmented Kalman Filter (AKF) is re-purposed, with as measurements the reference strains to replicate and as model the model of the scaled bearing. As a result, the AKF estimates a load which reproduces the reference strains when applied to the scaled bearing. This is demonstrated numerically on the use-case of testing a 3.4MW WT pitch bearing for ring fracture at an outer ring bolt hole using a 1.5MW WT pitch bearing test-rig.

1 Introduction

This article proposes an approach to determine the loads to apply during down-scaled testing of wind turbine (WT) pitch bearings. WTs are playing an important role in the transition towards renewable sources of energy, and are becoming more and more competitive in terms of Levelized Cost of Energy as they scale up in nameplate rating and size. In terms of geometry, this scaling up translates to three types of WT bearings in particular: the main bearing, which connects the rotor to the nacelle, the yaw bearing, which connects the nacelle to the tower, and finally the pitch bearings, which connect the blades to the rotor and allow for rotation about the longitudinal axis of the blade to adjust the angle of attack. These bearings are now reaching unprecedented dimensions to accommodate the size and weight of the connected components as well as the wind-generated forces. New designs, materials and manufacturing techniques are used to tackle those larger dimensions and design loads, but this novelty comes with many unknowns and requires extensive validation.

This article concerns itself with pitch bearings specifically. In addition to the above-presented unknowns resulting from their extraordinary size—more than 5m in diameter for 15MW offshore WTs [1]—, these bearings present unique challenges due to their limited range of motion, their periodic loading and ultimately, their resulting failure modes. Because of these particularities, the knowledge accumulated from more common bearing applications cannot be relied on [2].

These specificities make essential the experimental characterization and validation of bearings for WT applications, but full-size testing of large bearings is lengthy and expensive. Fixed costs include the test-rig itself, which is limited to a range of bearing sizes, as well as adequately-scaled infrastructure and specialized equipment for assembly and disassembly. Testing a single bearing takes up to 20 weeks and the costs of each run include the bearing under test itself, as well as man-hours for assembly and disassembly. Moreover, all of

these costs scale with the size of the bearing under test. Test-rigs in particular are extremely expensive and as bearing sizes increase, the existing test-rigs must be upgraded or new, larger test-rigs must be commissioned.

For the reasons listed above, a trend is emerging in the industry to down-scale tests with the goal of using smaller test-bearings during the design and validation of new larger bearings [3, 4, 5]. This makes experimental testing more affordable and reduces the need for expensive, full-size test-rigs by relying on already existing, smaller test-rigs. However, this also brings up the question of which loads to apply on the down-scaled bearing so that the test reproduces the fatigue life and defect formation of the larger reference bearing in operation. There is no established standard for this and manufacturers use proprietary methods to determine the loads for down-scaled testing [2].

The question raised above directly leads to the problem statement for the work presented in this article, which follows. Given a reference bearing and its associated design loads, given a failure mode of interest, and given a scaled bearing under test, this article proposes a method to derive the loads that should be applied on the scaled bearing to replicate the behavior of the reference bearing in terms of the failure mode of interest. This supposes the availability of a good enough model for the reference and for the scaled bearing as well as for the hubs that house them, and some knowledge on the most likely and/or critical failure modes. These assumptions are not trivial but are expected to be met when designing incrementally larger and larger pitch bearings.

This article is organized as follows. Section 2 elaborates further on this problem statement and provides details of the use-case considered in this work. This leads to section 3 which presents the proposed approach. This approach is numerically demonstrated on the pitch bearing use-case and the simulation results are discussed in section 4. Finally, section 5 summarizes our work and suggests further developments.

2 Detailed Problem Statement

This work considers as numerical proof-of-concept the down-scaled testing of a 3.4MW WT pitch bearing using a 1.5MW WT pitch bearing. These are denoted as the reference bearing and the scaled bearing, respectively. Table 1 summarizes some of their relevant specifications.

	Reference Bearing	Scaled Bearing
WT nameplate capacity	3.4MW	1.5MW
Type	Double-row 4-points-of-contact	Double-row 4-points-of-contact
Pitch diameter	2500mm	1931mm
Number of Rolling Elements (RE)	112	131
RE diameter	60mm	40mm
Conformity (μ)	0.52	0.525

Table 1: Specifications of the reference and scaled bearing (Laulagun bearing manufacturer)

2.1 Bearing Model

The reference bearing and the scaled bearing as well as their respective hubs are both modeled as follows. An analytical model of the ball bearing is combined with a finite element (FE) model of the hub to obtain field variables (displacements, strains, accelerations, ...) on the hub as a response to the forces and torques exerted by the blade on the inner ring of the pitch bearing [6, 7].

The ball bearing is a very non-linear element, as it distributes the inner ring load onto contact patches on the outer ring through the rolling elements. The abrupt changes in which rolling elements are under load and the associated contact mechanics for the active rolling elements introduce strong non-linearities. This is why scaling the loads for down-scaled testing by a constant factor does not result in representative outcomes, and why a more careful approach such as the one presented here is necessary. This will be demonstrated further in section 4.

Focusing back on the modeling proper, an analytical bearing model based on Hertzian contact theory is used to describe the interactions between the rolling elements and the raceways. First, the relative displacement of the bearing rings is computed. This displacement must result in bearing reaction forces that balance the load applied by the blade on the inner ring. Then, based on this relative displacement of the bearing rings, the analytical

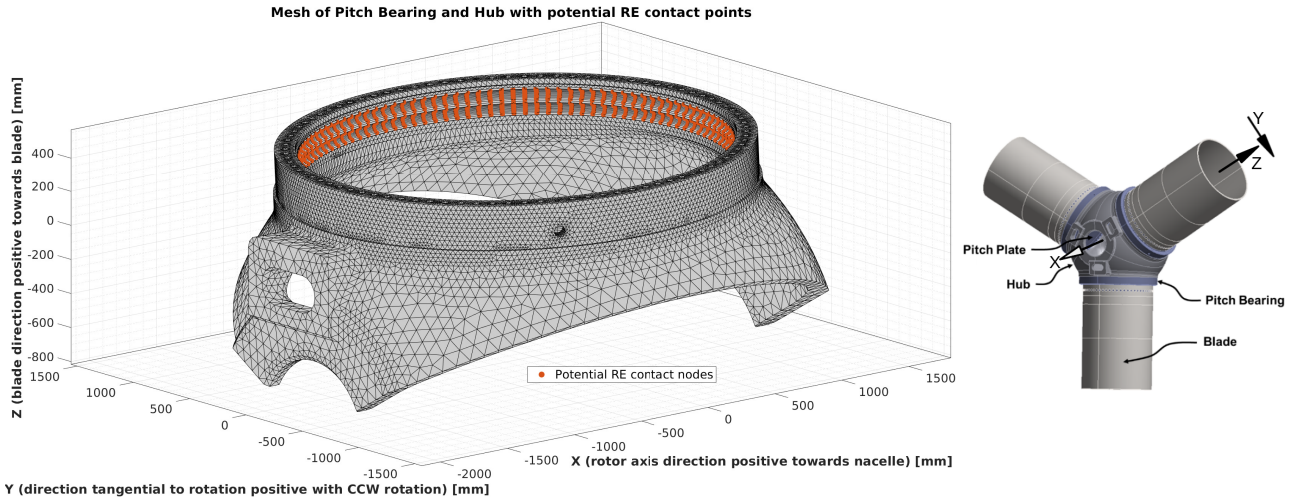

Figure 1: FE Model of reference bearing and hub, with potential RE contact points indicated in red, where the raceway forces are applied. On the right, the coordinate system of the bearing is put in context of the whole turbine for the top right pitch bearing. X points horizontally towards the nacelle, Y points tangentially in the direction of rotation, and Z points in the longitudinal direction of the blade away from the hub.

contact model computes the distribution of these bearing reaction forces through the rolling element contact patches over the outer raceways [6].

Finally, the hub is modeled using a reduced-order model based on FE Analysis, which uses those raceway forces as input. The dimensionality reduction is useful for virtual sensing because it makes the size of the state to estimate manageable, and because it makes the bearing observable for a feasible number of sensors [7]. The FE model of the bearing and hub is depicted in Figure 1, which also shows the coordinate system attached to the bearing used in this work. X points horizontally towards the nacelle, Y points tangentially in the direction of rotation, and Z points in the longitudinal direction of the blade away from the hub. Combined with the analytical contact model, this FE-based reduced-order model allows to compute at any point of the bearing and hub the strains resulting from the blade loads applied on the inner ring of the bearing.

2.2 Operating Loads and Resulting Failure Modes

Figure 2 shows these blade loads during typical operation of the 3.4MW WT, using the coordinate system defined in Figure 1. These are the loads considered throughout this work. Figure 2 shows that the Y and Z forces

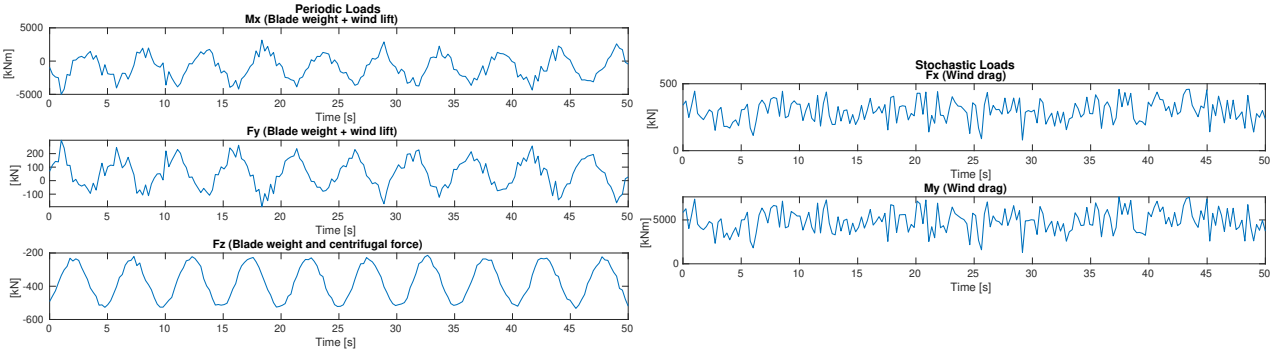

Figure 2: Operating loads on the 3.4MW WT pitch bearing. The dominantly-periodic components are grouped on the left and the stochastic components on the right.

as well as the X torque are dominantly periodic. This is due to the contribution of the weight of the blade as it rotates around the hub. On the other hand, the X force and Y torque are due to the drag as the wind passes over the blade, and the variations are stochastic. The periodicity of the loads, along with the small amplitude back and forth rotation of the pitch bearing (referred to as oscillations in literature and in the rest of this article), are the reasons why pitch bearings have particular failure modes and a reduced fatigue life.

The traditional approaches used to determine the fatigue life of continuously rotating bearings cannot be applied to pitch bearings because they oscillate with limited amplitude. Song and Karikari-Boateng extensively cover this in [2]. They show time-series data from an aeroelastic simulation of the 7MW Levenmouth Demonstration Turbine operated by ORE Catapult, with the design load cases prescribed by BS EN 61400-1 [8]. Song and Karikari-Boateng statistically demonstrate the small oscillation amplitude of the pitch bearing (<10° more than 99.5% of the time) and describe how this accelerates fatigue. The first reason is that the volume of stressed material in the bearing raceway decreases with the oscillation amplitude, which leads to higher damage accumulation per cycle. A second reason is that below a certain oscillation amplitude, the segment of raceway contacted by one rolling element throughout the oscillation does not overlap with the segment contacted by the adjacent rolling element. Below this critical amplitude, lubricant is likely to be pushed out of the contact area, which leads to mixed or boundary lubrication, and ultimately results in oscillation wear. Finally, Song and Karikari-Boateng list the common failure modes of pitch bearings that result from the particularities above. Amongst those failure modes, this work focuses on ring fracture resulting from cracks initiated at a bolt hole, as depicted in figure 3. More precisely, the failure mode of interest is ring fracture at a particular bolt hole, as

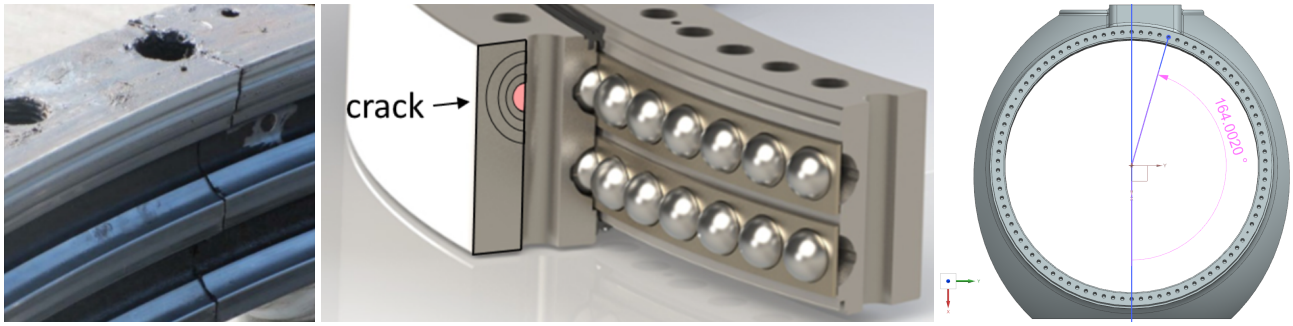

Figure 3: Example of actual ring fracture at bolt hole of a pitch bearing (Source: Romax Technology), crack initiation mechanism and location of the specific bolt hole considered in this work

indicated on the right of figure 3. This bolt hole was chosen based on experience accumulated with bearings already deployed in the field and based on the knowledge of the region of the bearing that receives the largest strains during operation of the WT.

The goal is thus to determine the loads to apply on the scaled bearing to replicate how this particular failure mode of interest develops on the reference bearing under the operating loads presented above. To this end, we propose to use load estimation techniques and, as measurements, to use the strains at key locations that should be preserved by the down-scaling of the test. This is presented in the next section.

3 Approach

The central idea in this work is to re-purpose load estimation techniques to determine the loads to apply during down-scaled testing of bearings. Load estimation using Augmented Kalman Filtering (AKF) is a very active topic in structural and mechanical applications [9, 10, 11, 12, 13], as well as in bearing applications more specifically [14]. This article will not present the detailed derivations of an (A)KF as this topic is very well covered in literature [7, 15, 16, 9], but the notational conventions are introduced below.

3.1 Augmented Kalman Filtering and Associated Notations

The underlying dynamical system is modeled in the discrete time using the traditional set of equations (1), where the system matrices may potentially be the result of local linearization around the current state $\mathbf{x}(k)$.

$$\begin{cases} \mathbf{x}(k+1) = \mathbf{A}\mathbf{x}(k) + \mathbf{B}\mathbf{u}(k) + \mathbf{w}(k), & \mathbf{w} \sim \mathcal{N}(\mathbf{0}, \mathbf{Q}) \\ \mathbf{y}(k) = \mathbf{H}\mathbf{x}(k) + \mathbf{D}\mathbf{u}(k) + \mathbf{v}(k), & \mathbf{v} \sim \mathcal{N}(\mathbf{0}, \mathbf{R}) \end{cases} \tag{1}$$

In (1), $\mathbf{A}$ and $\mathbf{B}$ describe the dynamics of the system, $\mathbf{H}$ and $\mathbf{D}$ how the system is observed, and $\mathbf{Q}$ and $\mathbf{R}$ the uncertainties on the input and modeled dynamics (through $\mathbf{w}(k)$) and on the measurements (through $\mathbf{v}(k)$), respectively.

Augmented Kalman Filtering consists in augmenting the system state $\mathbf{x}(k)$ with the input $\mathbf{u}(k)$, so that the input is part of the estimated state. This results in the augmented state-space model (2).

$$\begin{cases} \begin{bmatrix} \mathbf{x}(k+1) \\ \mathbf{u}(k+1) \end{bmatrix} = \begin{bmatrix} \mathbf{A} & \mathbf{B} \\ \mathbf{0} & \mathbf{I} \end{bmatrix} \begin{bmatrix} \mathbf{x}(k) \\ \mathbf{u}(k) \end{bmatrix} + \begin{bmatrix} \mathbf{w}(k) \\ \mathbf{w_u}(k) \end{bmatrix} \\ \mathbf{y}(k) = \begin{bmatrix} \mathbf{H} & \mathbf{D} \end{bmatrix} \begin{bmatrix} \mathbf{x}(k) \\ \mathbf{u}(k) \end{bmatrix} + \mathbf{v}(k) \end{cases} \tag{2}$$

which is condensed using the following substitutions:

$$\mathbf{x}^* = \begin{bmatrix} \mathbf{x} \\ \mathbf{u} \end{bmatrix}, \quad \mathbf{A}^* = \begin{bmatrix} \mathbf{A} & \mathbf{B} \\ \mathbf{0} & \mathbf{I} \end{bmatrix}, \quad \mathbf{w}^* = \begin{bmatrix} \mathbf{w} \\ \mathbf{w_u} \end{bmatrix} \quad \mathbf{w}^* \sim \mathcal{N}(\mathbf{0}, \mathbf{Q}^*), \quad \mathbf{H}^* = \begin{bmatrix} \mathbf{H} & \mathbf{D} \end{bmatrix}$$

$\mathbf{x}^*$ is the augmented state estimated by the AKF. Matrices $\mathbf{A}^*$ and $\mathbf{H}^*$ are used as the state prediction matrix and measurement matrix of the AKF, respectively. $\mathbf{R}$ is the covariance matrix of the uncertainty on the measurements. $\mathbf{Q}^*$ is the covariance matrix of the uncertainty on the input and on the dynamics of the system. In the AKF case, it represents the input dynamics, which is different than in the KF case. Indeed, in the augmented model (2), $\mathbf{w_u}$ is solely responsible for changes in $\mathbf{u}$, which is otherwise modeled as constant. This stems from the first fundamental assumption behind an AKF: the dynamics of the unknown input in (2) are modeled as a Gaussian random walk associated with covariance matrix $\mathbf{Q_{uu}}$, as indicated in (3) [15].

$$\mathbf{w_u} \sim \mathcal{N}(\mathbf{0}, \mathbf{Q_{uu}}) \tag{3}$$

The second assumption is that the modeling uncertainty, represented by $\mathbf{Q}$ in (1), is insignificant compared to the dynamics of the unknown input, captured by $\mathbf{Q_{uu}}$ in (3). This is required for input estimation to be feasible and to ensure that the measurement innovation—the difference between the actual measurement $\mathbf{y}(k)$ and the predicted measurement $\hat{\mathbf{y}}(k)$—results in an update in the estimated input and is not wrongly attributed to model mismatch. These prerequisites for input estimation using an AKF allow to approximate $\mathbf{Q}^*$ as in (4).

$$\mathbf{Q}^* = \begin{bmatrix} \mathbf{0} & \mathbf{0} \\ \mathbf{0} & \mathbf{Q_{uu}} \end{bmatrix} \tag{4}$$

This simplified structure is practical in the sense that it eliminates the tuning of $\mathbf{Q}$ in (1), but tuning $\mathbf{Q_{uu}}$ remains a challenge, especially as modelling the unknown input $\mathbf{u}(k)$ as a gaussian random walk is a strong assumption that rarely completely fits the actual input. As a result, tuning $\mathbf{Q_{uu}}$ is a compromise between the response delay of the estimator and its sensitivity to noise. $\mathbf{Q_{uu}}$ must be chosen based on which aspects of the input $\mathbf{u}(k)$ must be captured by the estimator [17].

With these notations introduced, the next subsection presents how this work re-purposes an AKF to determine the loads to apply during down-scaled testing of bearings.

3.2 Load Down-Scaling using Augmented Kalman Filtering

The original idea of this work is to change the role and meaning of the measurement of the AKF in order to determine the loads to apply during down-scaled testing of bearings. Instead of real measurements acquired in the physical world using actual sensors, the AKF takes as input reference measurements that must be reproduced during down-scaled testing. For the use-case of this article, this is implemented as summarized in figure 4. First, a simulation is run of the reference bearing in operation, using the model and loads presented above. From this simulation, strains on the raceways and near the bolt hole of interest are extracted. These strains must be replicated during down-scaled testing and are referred to as reference measurements. These reference measurements are provided as input to an AKF that uses the model of the scaled bearing for its $\mathbf{A}^*$ and $\mathbf{H}$ matrices. Putting it all together, thanks to these choices, the load estimated by this AKF is the load which, when applied on the scaled bearing, reproduces the reference strains at the key locations on the raceways and around the bolt hole of interest expected during operation of the reference bearing. This estimated load answers the problem tackled by this work.

The goal of this approach is to take advantage of the models that are available to describe the bearing deformation in response to loads, while still resorting to experiments to capture the more complex aspects of

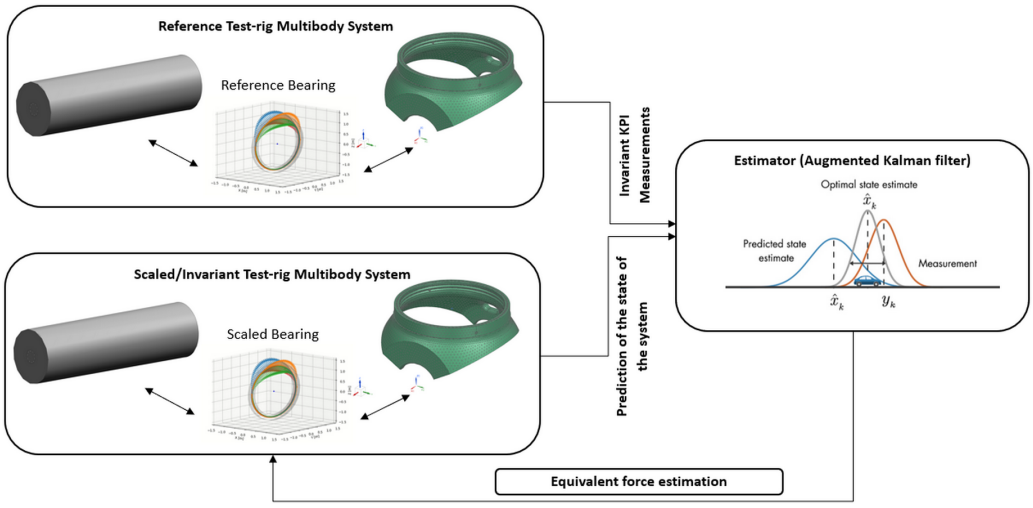

Figure 4: Schematic summary of the approach used in this work to determine loads for down-scaled testing

fatigue life and defect formation. This choice is made because the first step, predicting deformations from loads, is much less difficult to tackle numerically than the second step, predicting the number of cycles before failure due to cyclic deformations. Several methods exist to predict fatigue life, such as the stress- and strain-life approaches, rainflow cycle counting, and damage accumulation models. Unfortunately they all tend to generally introduce many challenges, approximations, and uncertainties [18]. In summary, the proposed approach numerically tackles the problem of reproducing strains during testing, because that can be done accurately, and still relies on down-scaled testing to collect fatigue life data, because fatigue life is difficult to accurately predict numerically.

This also points to a condition for this approach to produce representative results: beyond the reference strains at key locations, all other variables of the down-scaled testing must also be as close a possible to the reference bearing in operation. In particular, the materials, manufacturing processes and finer geometrical details that lead to stress concentrations or crack initiation must be kept identical because of their influence on defect formation and fatigue life. For example, replicating the operating conditions on a part with a different steel microstructure would still lead to misleading testing outcomes.

Coming back to the central idea of re-purposing an AKF to determine loads for down-scaled testing, this introduces two novelties. First, on a practical level, the AKF measurement $\mathbf{y}(k)$ is not limited by its feasibility in the physical world. This means that any relevant quantity can be used as reference measurement, even if it is impossible (stresses, forces, strains in the bulk material) or impractical (strains on the raceways or near a bolt hole) to measure. This is very useful as it allows down-scaled testing to preserve many different types of key quantities that must remain scale-invariant. Second, on a more conceptual level, this places this work at the intersection of control and estimation, with the AKF considered as a useful mathematical tool to solve the problem at hand. Instead of using measurements acquired on a given system to estimate the states and loads of that system, the approach presented here uses an AKF to determine the input to apply to that system in order to track some reference measurement.

The choice of an AKF to solve this tracking problem is motivated by two reasons. On a practical level, it is convenient because load estimation is a well covered topic for bearing applications, as argued in the introduction. In the wider context of developing bearings for high-value applications, it is expected that some estimator for bearing loads based on strain measurements is available or being developed independently anyway. This was the case for the use-case considered in this article [7], and it was advantageous to simply re-purpose the already available tools to determine the loads for down-scaled testing of WT pitch bearings. On a theoretical level, under the usual assumptions of a linear system with Gaussian noises, the optimality properties of a KF ensure that the proposed loads are good solutions to the down-scaling problem presented in this article. The next section elaborates further on this by showing results for the WT pitch bearing use-case considered here and by discussing the compromises of tuning the AKF.

4 Results

To demonstrate the approach presented above on the WT pitch bearing use-case, the proposed scaled loads are presented below, and the accuracy of the tracking of the reference strains is shown at one of the key locations.

4.1 Proposed Scaled Loads and Tracking of the Key Strains

Figure 5 illustrates in blue one of 10 strain signals that are provided as reference measurements to the AKF. These signals were generated by running a simulation of the 3.4MW WT pitch bearing under the operating loads

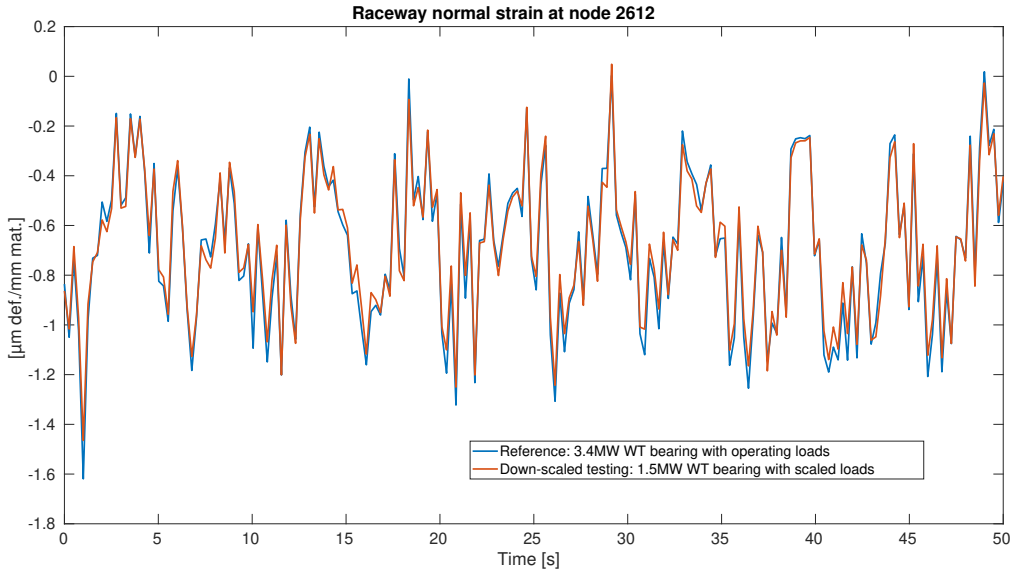

Figure 5: Raceway normal strain at one of the 10 key locations: comparison of reference bearing under operating load and scaled bearing under scaled load

presented earlier in subsection 2.2.

With these reference measurements, the AKF estimates scaled loads which, when applied on the 1.5MW WT pitch bearing, replicate these key strains, as shown in red on figure 5. This shows that the strains at the chosen key locations are indeed replicated during down-scaled testing. The tracking accuracy can be tuned and some slack is required to obtain realistic scaled loads, as discussed in the second part of this section.

Figures 6-8 show the proposed scaled loads in red and compare them to the reference operating loads in blue, and to loads scaled by a constant factor based on the ratios of dimensions and WT nameplate rating, in green. As expected, the scaled loads are indeed lower in magnitude and amplitude than the reference loads. They approach the loads scaled by a constant factor, but are still significantly different. This is understandable in light of the heavily non-linear nature of rolling element bearings, as mentioned earlier in subsection 2.1. Due to these non-linearities, a geometrical scaling of the bearing cannot be compensated by a constant scaling of the loads to keep the deformations invariant. This demonstrates that a more targeted approach such as the one presented here results in more representative outcomes from down-scaled testing and is actually necessary.

Figures 6-8 also show that the periodicity of the Y and Z component is preserved thanks to the information contained in the reference measurements, and without the need to explicitly enforce it. In summary, the proposed scaled loads correctly replicate the desired strains at key locations, while simultaneously remaining realistic and retaining the basic properties expected from WT pitch bearing loads.

The next subsection provides further considerations on the choice of the key locations at which these strain signals are taken, and on the tuning of the AKF.

4.2 Choice of Key Locations for Reference Strains and Tuning of the AKF

Going back to subsection 2.2, the goal of this work is to reproduce strains around the bolt hole where the failure mode of interest develops. As a result, 4 of the key locations are nodes directly surrounding that bolt hole. To ensure observability of the resulting load estimation problem, and to obtain realistic scaled loads, 6 additional

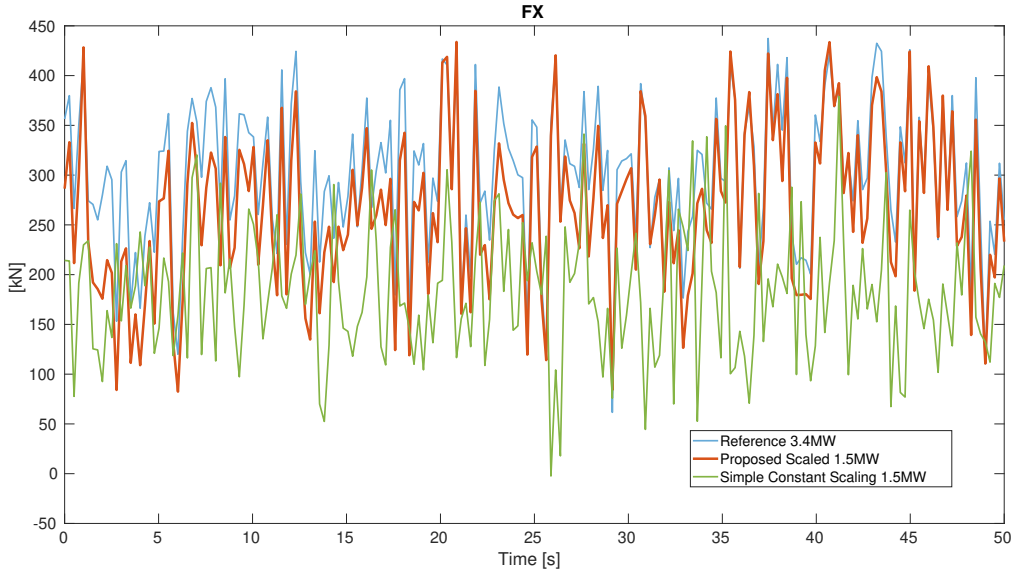

Figure 6: Proposed scaled X force, compared with reference force and force scaled by a constant factor

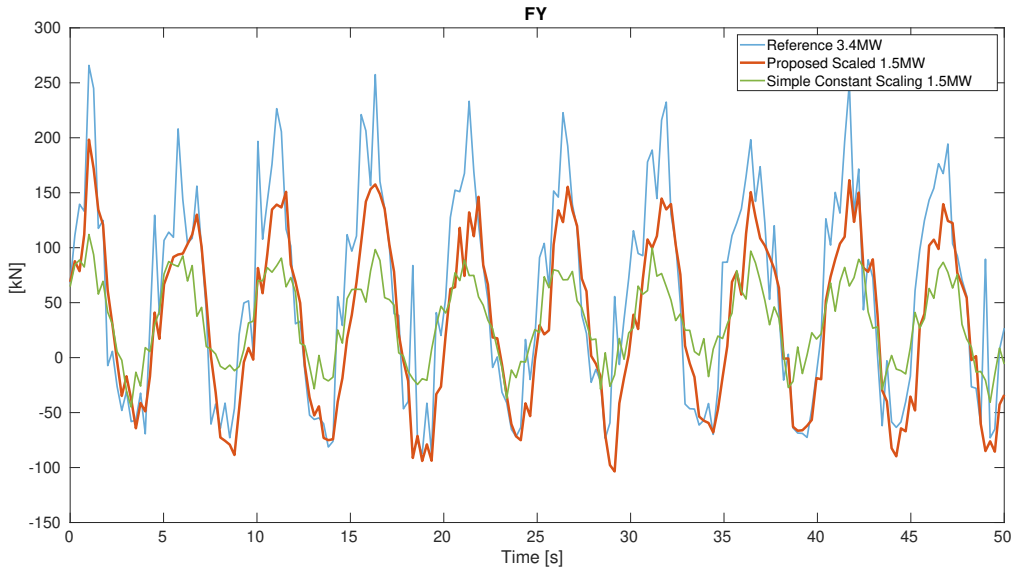

Figure 7: Proposed scaled Y force, compared with reference force and force scaled by a constant factor

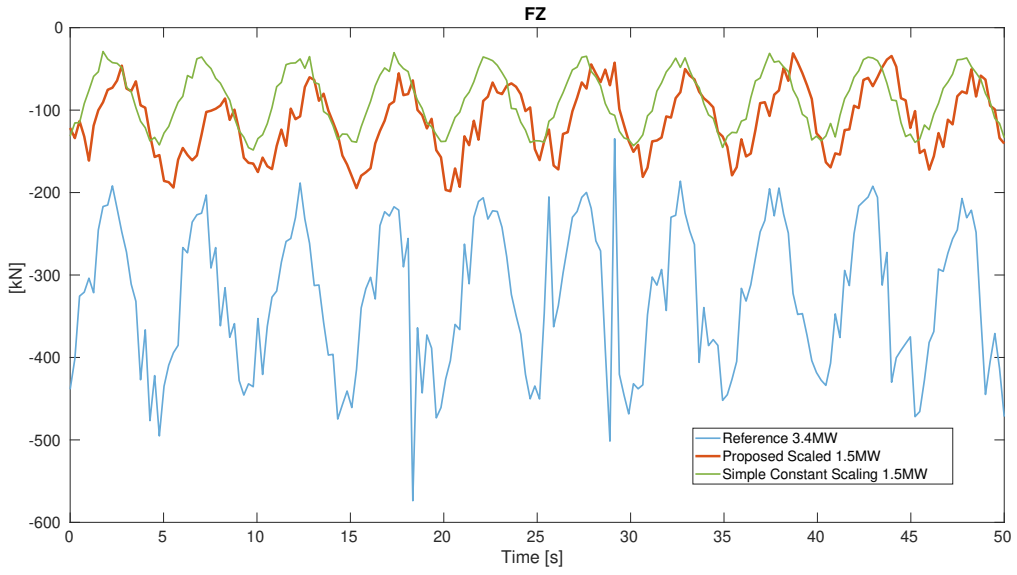

Figure 8: Proposed scaled Z force, compared with reference force and force scaled by a constant factor

key locations are picked on the outer raceways of the bearing, one of those locations is at the same angle as the bolt hole of interest (i.e. raceway position closest to bolt hole), the others are distributed around the bearing. Without those additional reference measurements that are not directly related to the failure mode of interest, tracking of the key strains around the bolt hole is still possible. However, the associated load estimation problem becomes ill-conditioned or even undetermined, and the resulting scaled loads, while numerically satisfying from a tracking point of view, are completely impractical and/or unrealistic. With the key strain locations picked in this work, the obtained scaled loads are still typical WT pitch bearing loads from a qualitative standpoint and can be practically implemented in down-scaled testing.

Tuning the AKF is a similar compromise between the tracking accuracy of the key strains, and the smoothness and feasibility of the resulting scaled loads. This tuning is defined by two matrices, $\mathbf{Q}^*$ and $\mathbf{R}$. As discussed earlier in subsection 3.1, only the $\mathbf{Q_{uu}}$ sub-block of $\mathbf{Q}^*$ is non-zero. It is the covariance matrix of the random walk model for the scaled loads that this work aims to determine. As a result, $\mathbf{Q_{uu}}$ controls how fast the scaled loads are allowed to change with time. Higher values correspond to more dynamical scaled loads with typically higher magnitudes. Regarding the $\mathbf{R}$ matrix, it takes on a different role than usual in this work which re-purposes the AKF to determine scaled loads. For classical estimation purposes, the $\mathbf{R}$ matrix describes the uncertainty on the measurements. Here, it controls how much slack is allowed in the tracking of the reference strains that must be replicated in down-scaled testing.

In this work, $\mathbf{R}$ is chosen as low as possible to ensure that the reference strains are replicated as accurately as possible. Some slack must be left though to avoid numerical artifacts in the scaled loads. $\mathbf{Q_{uu}}$ is chosen just high enough to allow for accurate tracking while still keeping the dynamics of the loads typical of a WT.

5 Conclusion

This article has shown how the AKF can be re-purposed to determine the loads to apply during down-scaled testing of bearings. As down-scaled testing of large bearings is becoming increasingly popular and economically necessary, this work aims to make this practice more rigorous and the results more reliable. The proposed approach allows to reproduce the loading cycles received during operation by the material around a specific failure mode. This is done by re-purposing an AKF, which allows to extract additional value from existing load estimation work. This work requires accurate enough bearing models and an informed choice of failure mode(s) to focus on, which are reasonable expectations when designing incrementally larger and larger pitch bearings.

This approach has been numerically demonstrated on the use-case of testing a 3.4MW WT pitch bearing using a 1.5MW WT pitch bearing test-rig. This article has shown how the reference strains are accurately replicated by the proposed scaled loads. The obtained loads remain typical of WT loads, and can be practically generated in testing. However, they are different from loads scaled by a constant factor based on the ratios of dimensions and WT nameplate rating. This demonstrates that this approach is essential to ensure the fidelity of down-scaled testing.

Our work can therefore allow to accelerate the development of WT pitch bearings and reduce the testing costs, while still obtaining representative test results in a rigorous manner. However, the proposed approach cannot entirely replace full-size testing, and it must be combined with good model fitting and proper experimental investigations at every scale, from material characterization of coupons, to final full-size validation, and to monitoring of deployed WTs. Future work should compare the experimental outcomes of full-size and down-scaled testing when using the load-scaling method presented in this article, and investigate if signals other than strains near the failure mode of interest could lead to more fidelity between full-size and down-scaled testing.

Acknowledgements

The European Commission is gratefully acknowledged for their support of the INNTERESTING research project (GA 851245) along with Internal Funds KU Leuven for their backing.

References

[1] Evan Gaertner, Jennifer Rinker, Latha Sethuraman, Frederik Zahle, Benjamin Anderson, Garrett E. Barter, Nikhar J. Abbas, Fanzhong Meng, Pietro Bortolotti, Witold Skrzypinski, George N. Scott, Roland Feil, Henrik Bredmose, Katherine Dykes, Matthew Shields, Christopher Allen, and Anthony Viselli. IEA Wind TCP Task 37: Definition of the IEA 15-Megawatt Offshore Reference Wind Turbine. Technical Report NREL/TP-5000-75698, National Renewable Energy Lab. (NREL), Golden, CO (United States), March 2020.

[2] Wooyong Song and K. A. Karikari-Boateng. Enhanced test strategy of pitch bearing based on detailed motion profile. *Forschung im Ingenieurwesen*, 85(4):973–983, Dec 2021.

[3] Kim Branner and Peter Berring. Methods for testing of geometrical down-scaled rotor blades. Technical Report E-0069, DTU Wind Energy, Roskilde, Denmark, 2014.

[4] Geraldo F. de S. Rebouças and Amir R. Nejad. On Down-Scaled Modelling of Wind Turbine Drivetrains. *Journal of Physics: Conference Series*, 1618(5):052008, September 2020.

[5] Fabian Schwack, Fabian Halmos, Matthias Stammler, Gerhard Poll, and Sergei Glavatskih. Wear in wind turbine pitch bearings—a comparative design study. *Wind Energy*, 25(4):700–718, 2022.

[6] J. Fiszer, T. Tamarozzi, B. Blockmans, and W. Desmet. A time-dependent parametric model order reduction technique for modelling indirect bearing force measurements. *Mechanism and Machine Theory*, 83:152–174, Jan 2015.

[7] Nathan Dwek, Bart Blockmans, Jan Croes, Bert Pluymers, and Matteo Kirchner. Sensor selection for load estimation of a wind turbine pitch bearing. In *Proceedings of ISMA 2022 International Conference on Noise and Vibration Engineering*, Heverlee, Sep 2022. KU Leuven - Department of Mechanical Engineering.

[8] Wind energy generation systems part 1: Design requirements. Standard BS EN IEC 61400-1, BSI, London, UK, 2019.

[9] E. Lourens, E. Reynders, G. De Roeck, G. Degrande, and G. Lombaert. An augmented Kalman filter for force identification in structural dynamics. *Mechanical Systems and Signal Processing*, 27:446–460, February 2012.

[10] B. Forrier, F. Naets, and W. Desmet. Broadband load torque estimation in mechatronic powertrains using nonlinear kalman filtering. *IEEE Transactions on Industrial Electronics*, 65(3):2378–2387, Mar 2018.

[11] R. Cumbo, T. Tamarozzi, K. Janssens, and W. Desmet. Kalman-based load identification and full-field estimation analysis on industrial test case. *Mechanical Systems and Signal Processing*, 117:771–785, February 2019.

[12] Enrico Risaliti, Tommaso Tamarozzi, Martijn Vermaut, Bram Cornelis, and Wim Desmet. Multibody model based estimation of multiple loads and strain field on a vehicle suspension system. *Mechanical Systems and Signal Processing*, 123:1–25, May 2019.

[13] Jelle Bosmans, Yon Vanommeslaeghe, Luk Geens, Jakob Fiszer, Jan Croes, Matteo Kirchner, Joachim Denil, Paul De Meulenaere, and Wim Desmet. Development and embedded deployment of a virtual load sensor for wind turbine gearboxes. *Journal of Physics: Conference Series*, 1618(2):022011, Sep 2020.

[14] Stijn Kerst, Barys Shyrokau, and Edward Holweg. A model-based approach for the estimation of bearing forces and moments using outer ring deformation. *IEEE Transactions on Industrial Electronics*, 67(1):461–470, Jan 2020.

[15] Robert Grover Brown and Patrick Y. C. Hwang. *Introduction to random signals and applied Kalman filtering: with MATLAB exercises and solutions*. Wiley, New York, 3rd ed edition, 1997.

[16] Dan Simon. *Optimal state estimation: Kalman, H [infinity] and nonlinear approaches*. Wiley-Interscience, Hoboken, N.J, 2006. OCLC: ocm64084871.

[17] T Tamarozzi, E Risaliti, W Rottiers, K Janssens, and W Desmet. Noise, ill-conditioning and sensor placement analysis for force estimation through virtual sensing. page 15.

[18] Joseph Edward Shigley, Charles R. Mischke, and Richard G. Budynas. *Mechanical engineering design*. McGraw-Hill series in mechanical engineering. McGraw-Hill, New York, NY, 7th ed edition, 2004.